Nonlinear, Large Deformation Finite-Element Beam/Column Formulation for the Study of the Human Spine: Investigation of the Role of Muscle on Spine Stability

Franck J. Vernerey[1] and Brian Moran[2]

Abstract: A nonlinear, large deformation beam/column formulation is used to model the behavior of the human spine under compressive load. The stabilizing roles of muscles are accounted for using Patwardhan's assumption that muscles act to direct the load along the tangent of the column. Three aspects of the spinal structure are then investigated. First, we look at the effects of two different assumptions for the action of muscles, leading to significant differences in the spine behavior. Second, the difference in mechanical properties between the vertebrae and the spinal disks is explored. Third, a nonlinear mechanical response of the spinal disk that arises from a two-step hierarchical homogenization technique is used. It is found that these factors have an important influence on the overall behavior of the spine structure. The present formulation offers a versatile model to investigate various features of the human spine, while remaining affordable computationally. It also provides an interesting framework for future multiscale studies of the human spine.

DOI: 10.1061/(ASCE)EM.1943-7889.0000176

CE Database subject headings: Bioengineering; Stability; Finite element method; Deformation; Beams; Columns.

Author keywords: Biomechanics; Stability; Nonlinear beam theory; Finite elements.

Introduction

Mathematical modeling of the human spine is critical to understand the mechanisms by which the structure keeps its stability and prevents damage. Furthermore, an accurate model provides a framework for virtual testing and measurements, which cannot be made from in vivo experiments and therefore is valuable to bring answers to the medical community.

The challenge in modeling the human spinal column resides in the fact that it is a very heterogeneous structure, from the scale of tissue microstructure to the entire column structure. While a computational model of the human spine that incorporates all the details is not feasible, an efficient and realistic model that can capture critical parameters is essential. In terms of efficiency, beam-column formulations represent a good alternative for the prediction of the behavior of the vertical column with a relatively few degrees of freedom. Thus, Kim and Kim (2004) used an Euler beam formulation that accounts for bending and Kiefer et al. (1997) examined the Timoshenko beam model that includes the effects of shear. However, to the knowledge of the authors, no studies have used a beam-column formulation accounting for the six degrees of freedom (namely, tension, two shear, torsion, and two bending) that a spine segment may experience. To improve this class of models, we propose two new developments. First, the use of Reissner's beam theory to account for all six degrees of freedom, and second, material properties of the beam are derived from the multiscale hierarchical methodology (Hao et al. 2004; Vernerey 2010), which consists of a step-by-step homogenization from small scale to large scale. This may provide a better understanding of the impact of small scale features that are present in the spinal structure on the overall structure.

Another challenge is in understanding and modeling the actions of muscles, as they are known to play an important role in the stabilization of the spinal column. This was investigated in Crisco and Panjabi (1992) and Crisco et al. (1992) in the case of compressive loading. Using both analytical and experimental approaches, they determined that the buckling compressive load of a human cadaveric spine without muscles was about 100 N, while the compressive load during normal activity usually reaches 1,000 N. To account for these observations, Patwardhan et al. (2001) introduced a model for the action of muscle in the frontal plane, based on the assumption that muscles tend to direct force along the tangent of the spine. This assumption showed satisfactory results but the model used in Patwardhan et al. (2001) remained extremely simplified.

This work aims at two things: One, developing an efficient model for the vertebral column and two, keeping the accuracy and information from the underlying multiscale structure. In particular, the objectives of this paper are as follows:

1. Develop a computational column model that accounts for the six degrees of freedom of the spinal column cross section, namely, shear strain in two directions, one tensile strain, bending in two directions, and torsion;
2. Compare the present model with previous studies on the lumbar spine and discuss two possible assumptions with regard

[1]Assistant Professor, Dept. of Civil, Environmental and Architectural Engineering, Univ. of Colorado at Boulder, Campus Box 428, Boulder, CO 80309-0428 (corresponding author). E-mail: franck.vernerey@colorado.edu

[2]Professor, Dept. of Civil and Environmental Engineering, Northwestern Univ., 2145 Sheridan Rd., Evanston, IL 60208-3111; and Dept. of Civil, Environmental and Architectural Engineering, Univ. of Colorado at Boulder, Campus Box 428, Boulder, CO 80309-0428.

Note. This manuscript was submitted on July 29, 2008; approved on March 23, 2010; published online on March 27, 2010. Discussion period open until April 1, 2011; separate discussions must be submitted for individual papers. This paper is part of the ***Journal of Engineering Mechanics***, Vol. 136, No. 11, November 1, 2010. ©ASCE, ISSN 0733-9399/2010/11-1319–1328/$25.00.

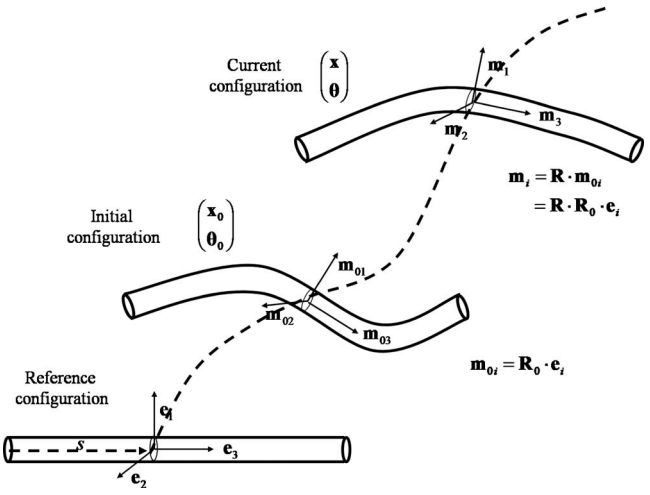

Fig. 1. Reference, initial, and current configurations of the beam

to the action of muscles: the tangent assumption and the secant assumption;

3. Use homogenization theory to determine the behavior of intervertebral disks from the knowledge of the response of soft tissues and geometry of the vertebrae; and
4. Reassess the frontal plane model for the lumbar spine with the presence of disks and vertebrae, gravity load, and nonlinear disk response for both the tangent assumption and the secant assumption.

The paper is organized as follows. In the next section, we introduce the beam-column formulation, derive the weak and strong forms of the governing equations, and present the finite-element discretization. In the "Homogeneous Column, Frontal Plane Model" section, after introducing the mechanical behavior of the column, we describe two models for the response of muscle, namely, the tangent and the secant models. We then reproduce the frontal plane model with muscle described by Patwardhan et al. (2001), compare results, and investigate differences between the two approaches. In the "Nonlinear Multiscale Spine Model with Disks" section, we describe a more realistic frontal plane model of the lumbar spine by including disks. We also derive the response of the column in bending from the hierarchical homogenization approach and discuss the implication of the new model. We finally discuss our results and potential research.

Three-Dimensional Reissner's Beam Theory for the Vertebral Column

Kinematics

Reissner's beam theory (Kapania and Li 2003; Reissner 1981; Simo 1985; Simo and Vu-Quoc 1986; Vernerey et al. 2007) gives a mathematical description of a beam column based on six degrees of freedom: three displacements and three rotations. Let us consider a beam in the Cartesian coordinate system $\mathbf{e}_i (i=1,2,3)$ for which the arc-length coordinate is given by the scalar s. The initial configuration of the beam is defined at point s by the position vector $\mathbf{x}_0(s)$ and three coordinate axes, $\mathbf{m}_{0i}(s)$, $(i=1,2,3)$ (oriented with the beam as depicted in Fig. 1). Instead of using the vector $\mathbf{m}_{0i}$, it is convenient to introduce an initial orthogonal rotation tensor $\mathbf{R}_0$ such that $\mathbf{m}_{0i}$ is interpreted as the rotated basis vector

$$\mathbf{m}_{0i} = \mathbf{R}_0 \cdot \mathbf{e}_i \tag{1}$$

The initial rotation tensor $\mathbf{R}_0$ can be written in terms of rotations in the three spatial directions represented by the vector $\boldsymbol{\theta}_0(s)$. A point in the initial configuration can then be described by two vectors: its position $\mathbf{x}_0(s)$ and its rotation $\boldsymbol{\theta}_0(s)$. Let us now consider the beam in its current configuration. The position and rotation of point s are now identified by the vectors $\mathbf{x}(s)$ and $\boldsymbol{\theta}(s)$, respectively. The coordinate axes $\mathbf{m}_i(s)$, $(i=1,2,3)$ can be found by rotating the initial vectors $\mathbf{m}_{0i}(s)$, $(i=1,2,3)$ with the current rotation tensor $\mathbf{R}$ as follows:

$$\mathbf{m}_i = \mathbf{R} \cdot \mathbf{m}_{0i} \tag{2}$$

This can equivalently be written in terms of the basis vector using Eqs. (1) and (2) as follows:

$$\mathbf{m}_i = \mathbf{R} \cdot \mathbf{R}_0 \cdot \mathbf{e}_i \tag{3}$$

In the spatial configuration, the finite strains are given by

$$\boldsymbol{\varepsilon} = \mathbf{x}_{,s} - \mathbf{m}_3 \tag{4}$$

where $\mathbf{x}_{,s} = \partial\mathbf{x}/\partial s$. The bending and torsion strains are given with the skew-symmetric curvature tensor as follows:

$$\mathbf{K} = \mathbf{R}_{,s} \cdot \mathbf{R}^T \tag{5}$$

Similarly, the curvature tensor $\mathbf{K}$ can be represented by an axial vector $\boldsymbol{\kappa}$ that contains the three curvature parameters

$$\boldsymbol{\kappa} = \begin{bmatrix} -K_{23} & K_{13} & -K_{12} \end{bmatrix}^T \tag{6}$$

The material strain fields are then found by rotating the frame back to the reference frame

$$\boldsymbol{\varepsilon}^M = (\mathbf{R}\cdot\mathbf{R}_0)^T \cdot \boldsymbol{\varepsilon} \quad \text{and} \quad \boldsymbol{\kappa}^M = (\mathbf{R}\cdot\mathbf{R}_0)^T \cdot \boldsymbol{\kappa} \tag{7}$$

Virtual Internal Work

The internal energy of the beam of material and current length L and L^M, respectively, and material and current cross sections $A(s)$ and $A^M(s)$, respectively, is written as follows:

$$W_{\text{int}} = \int_L A(s)(\mathbf{n}\cdot\boldsymbol{\varepsilon} + \mathbf{m}\cdot\boldsymbol{\kappa})ds = \int_{L^M} A^M(s)(\mathbf{n}^M\cdot\boldsymbol{\varepsilon}^M + \mathbf{m}^M\cdot\boldsymbol{\kappa}^M)ds \tag{8}$$

where the quantities $\mathbf{n}$ and $\mathbf{m}$ = stresses and moments in the current configuration and $\mathbf{n}^M$ and $\mathbf{m}^M$ = stresses and moments in the material configuration. It is straightforward to show that

$$\mathbf{n}^M = (\mathbf{R}\cdot\mathbf{R}_0)^T\cdot\mathbf{n} \quad \text{and} \quad \mathbf{m}^M = (\mathbf{R}\cdot\mathbf{R}_0)^T\cdot\mathbf{m} \tag{9}$$

The governing equations are then derived by applying the principle of virtual work. Let us first note that the virtual rotation vector $\delta\mathbf{R}$ is written as

$$\delta\mathbf{R} = \delta\mathbf{W}\cdot\mathbf{R} \tag{10}$$

where $\delta\mathbf{W}$ = vector of infinitesimal rotation superposed on the rotation $\mathbf{R}$. Because $\delta\mathbf{W}$ is skew symmetric, it can be replaced with its axial vector $\delta\mathbf{w}$. Let us now consider the virtual work δW that arises from the virtual displacement $\delta\mathbf{x}$ and rotation $\delta\mathbf{w}$ as follows:

J. Eng. Mech., 2010, 136(11): 1319-1328

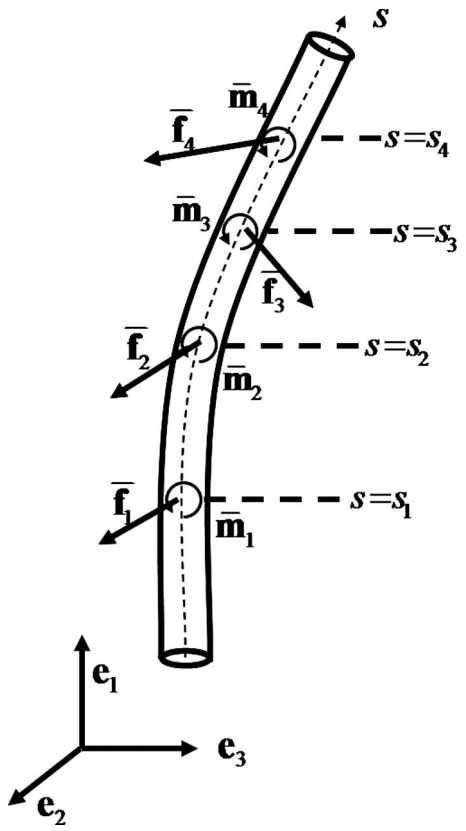

Fig. 2. Muscle forces and moments

$$\delta W_{\text{int}} = \int_L A(s)(\mathbf{n}\cdot\delta\boldsymbol{\varepsilon} + \mathbf{m}\cdot\delta\boldsymbol{\kappa})ds \tag{11}$$

One can show that the virtual material strains have the following form:

$$\delta\boldsymbol{\varepsilon}^M = (\mathbf{R}\cdot\mathbf{R}_0)^T\cdot[\delta\mathbf{x}_{,s} + \mathbf{x}_{,s}\times\delta\mathbf{w}]$$
$$\delta\boldsymbol{\varepsilon} = (\mathbf{R}\cdot\mathbf{R}_0)\cdot\delta\boldsymbol{\varepsilon}^M = \delta\mathbf{x}_{,s} + \mathbf{x}_{,s}\times\delta\mathbf{w}$$

$$\delta\boldsymbol{\kappa}^M = (\mathbf{R}\cdot\mathbf{R}_0)^T\cdot[\delta\mathbf{w}_{,s}] \quad \delta\boldsymbol{\kappa} = (\mathbf{R}\cdot\mathbf{R}_0)\cdot\delta\boldsymbol{\kappa}^M = \delta\mathbf{w}_{,s} \tag{12}$$

Using Eqs. (11) and (12), the virtual work can be rewritten as

$$\delta W_{\text{int}} = \int_L A(s)[\mathbf{n}\cdot\delta\mathbf{x}_{,s} - (\mathbf{x}_{,s}\times\mathbf{n})\cdot\delta\mathbf{w} + \mathbf{m}\cdot\delta\mathbf{w}_{,s}]ds \tag{13}$$

Virtual External Work

The external work is decomposed into two parts: the work exerted by muscles and the work exerted by external loads. We assume that muscles act on the vertebral column in the form of point forces $\bar{\mathbf{f}}_I$ and moments $\bar{\mathbf{m}}_I$ acting at point $s=s_I$, as depicted in Fig. 2. The virtual work δW_{mus} exerted by muscle forces and moments when the column is subject to the virtual displacement $\delta\mathbf{x}$ and rotation $\delta\mathbf{w}$ is simply written as

$$\delta W_{\text{mus}} = \sum_{I=1}^{N}[\bar{\mathbf{f}}_I\cdot\delta\mathbf{x}(s_I) + \bar{\mathbf{m}}_I\cdot\delta\mathbf{w}(s_I)]$$
$$= \int_L\left\{\sum_{I=1}^{N}[\delta(s_I - s)\bar{\mathbf{f}}_I\cdot\delta\mathbf{x} + \Delta(s_I - s)\bar{\mathbf{m}}_I\cdot\delta\mathbf{w}]\right\}ds \tag{14}$$

where N=number of muscles and Δ=function such that

$$\Delta(x) = \begin{cases} 1 & x = 0 \\ 0 & x \neq 0 \end{cases} \tag{15}$$

Finally, the external load contains gravitation forces due to the weight of the column and traction forces on both ends of the column

$$\delta W_{\text{ext}} = \int_L A(s)\rho\mathbf{g}\cdot\delta\mathbf{x}ds + \mathbf{t}\cdot\delta\mathbf{x} + \mathbf{c}\cdot\delta\mathbf{w}|_{\Gamma_t} \tag{16}$$

where ρ=current mass density; $\mathbf{g}$=gravity vector; and $\mathbf{t}$ and $\mathbf{c}$ =current force and couple, respectively, on the traction boundary Γ_t.

Principle of Virtual Work and Governing Equations

The principle of virtual work states that the total virtual work must vanish for any virtual displacement $\delta\mathbf{x}$ and rotation $\delta\mathbf{w}$. Thus, we have

$$\delta W_{\text{int}} - \delta W_{\text{mus}} - \delta W_{\text{ext}} = 0 \quad \text{for all } (\delta\mathbf{x}, \delta\mathbf{w}) \tag{17}$$

Substituting Eqs. (13), (14), and (16) in Eq. (17) and using the divergence theorem lead to the following equation:

$$\int_L\left(\left\{-A(s)\mathbf{n}_{,s} - A(s)\rho\mathbf{g} - \sum_{I=1}^{N}[\Delta(s_I - s)\bar{\mathbf{f}}_I]\right\}\cdot\delta\mathbf{x}\right)ds$$
$$+\int_L\left(A(s)\left\{(-\mathbf{x}_{,s}\times\mathbf{n} - \mathbf{m}_{,s}) - \sum_{I=1}^{N}[\Delta(s_I - s)\bar{\mathbf{m}}_I]\right\}\cdot\delta\mathbf{w}\right)ds$$
$$+[(A\mathbf{n} - \mathbf{t})\cdot\delta\mathbf{x} + (A\mathbf{m} - \mathbf{c})\cdot\delta\mathbf{w}]|_{\Gamma_t} = 0 \tag{18}$$

where A=cross section of the column at the boundary Γ_t. This is the weak form of the governing equations. The strong form of the governing equations for the stress $\mathbf{n}$ and moment $\mathbf{m}$ in the column follows directly

$$A(s)(\mathbf{n}_{,s} + \rho\mathbf{g}) + \sum_{I=1}^{N}[\delta(s_I - s)\bar{\mathbf{f}}_I] = \mathbf{0}$$

$$A(s)(\mathbf{m}_{,s} + \mathbf{x}_{,s}\times\mathbf{n}) + \sum_{I=1}^{N}[\delta(s_I - s)\bar{\mathbf{m}}_I] = \mathbf{0} \tag{19}$$

The boundary conditions in the current configuration are written as

$$A\mathbf{n} = \mathbf{t} \quad \text{and} \quad A\mathbf{m} = \mathbf{c} \quad \text{on } \Gamma_t \tag{20}$$

Computational Aspects

The finite-element method is used to solve the beam/column equations. The continuum fields $\mathbf{x}$ and $\mathbf{w}$, and the virtual fields $\delta\mathbf{x}$ and $\delta\mathbf{w}$ are written in terms of their nodal values $\mathbf{x}^\alpha$, $\mathbf{w}^\alpha$, $\delta\mathbf{x}^\alpha$, and $\delta\mathbf{w}^\alpha$ and the shape function N^α as follows:

J. Eng. Mech., 2010, 136(11): 1319-1328

$$\mathbf{x}(s)=\sum_{\alpha=1}^{nn} N^{\alpha}(s)\mathbf{x}^{\alpha} \quad \text{and} \quad \delta\mathbf{x}(s)=\sum_{\alpha=1}^{nn} N^{\alpha}(s)\delta\mathbf{x}^{\alpha}$$

$$\mathbf{w}(s)=\sum_{\alpha=1}^{nn} N^{\alpha}(s)\mathbf{w}^{\alpha} \quad \text{and} \quad \delta\mathbf{w}(s)=\sum_{\alpha=1}^{nn} N^{\alpha}(s)\delta\mathbf{w}^{\alpha} \tag{21}$$

By using these relations in Eqs. (13), (14), and (16), we can develop expressions for the nodal internal force, muscle force, and external forces. Let us assume that the cross section area remains constant during deformation, ($A=A^M$), and introduce $\mathbf{u}^{\alpha}=\begin{bmatrix}\mathbf{x}^{\alpha}\\ \mathbf{w}^{\alpha}\end{bmatrix}$. The finite-element discretized forms for energy and forces take the form

$$\begin{cases}\delta W_{\text{int}}=\sum_{\alpha=1}^{nn}\delta\mathbf{u}^{\alpha}\cdot\mathbf{f}_{\text{int}}^{\alpha}\\ \delta W_{\text{mus}}=\sum_{\alpha=1}^{nn}\delta\mathbf{u}^{\alpha}\cdot\mathbf{f}_{\text{mus}}^{\alpha} \quad \text{where}\\ \delta W_{\text{ext}}=\sum_{\alpha=1}^{nn}\delta\mathbf{u}^{\alpha}\cdot\mathbf{f}_{\text{ext}}^{\alpha}\end{cases}$$

$$\begin{cases}\mathbf{f}_{\text{int}}^{\alpha}=\int_L A\left\{N_{,s}^{\alpha}\mathbf{n} \quad N_{,s}^{\alpha}\mathbf{m}+N^{\alpha}\left[\left(\sum_{\gamma=1}^{nn}N_{,s}^{\gamma}\mathbf{x}^{\gamma}\right)\times\mathbf{n}\right]\right\}^T ds\\ \mathbf{f}_{\text{mus}}^{\alpha}=\int_L\left[N^{\alpha}\delta(s_I-s)\bar{\mathbf{f}}_I \quad N^{\alpha}\delta(s_I-s)\bar{\mathbf{m}}_I\right]^T ds\\ \mathbf{f}_{\text{ext}}^{\alpha}=\int_L A\left[N^{\alpha}\rho\mathbf{g} \quad \mathbf{0}\right]^T ds\end{cases} \tag{22}$$

The equilibrium at node α follows directly from Eq. (17) as

$$\mathbf{f}_{\text{int}}^{\alpha}=\mathbf{f}_{\text{mus}}^{\alpha}+\mathbf{f}_{\text{ext}}^{\alpha} \tag{23}$$

The parametrization of the finite rotation is based on the rotation vector $\boldsymbol{\theta}(s)$ as described by Ibrahimbegović et al. (1995). The relationship between $\boldsymbol{\theta}$ and the total rotation tensor $\mathbf{R}\cdot\mathbf{R}_0$ is given by the Rodriguez formula

$$\mathbf{R}\cdot\mathbf{R}_0=\cos\theta\mathbf{I}+\frac{\sin\theta}{\theta}\boldsymbol{\Theta}+\frac{1-\cos\theta}{\theta^2}\boldsymbol{\theta}\times\boldsymbol{\theta} \tag{24}$$

where $\theta=\sqrt{\boldsymbol{\theta}\cdot\boldsymbol{\theta}}$ and

$$\boldsymbol{\Theta}=\begin{bmatrix}0 & -\theta_3 & \theta_2\\ \theta_3 & 0 & -\theta_1\\ -\theta_2 & \theta_1 & 0\end{bmatrix}$$

The infinitesimal rotation $\delta\mathbf{w}$ is related to the variation of rotation angle $\delta\boldsymbol{\theta}$ through the tensor $\mathbf{T}$ as follows:

$$\delta\mathbf{w}=\mathbf{R}\cdot\mathbf{R}_0\cdot\mathbf{T}(\boldsymbol{\theta})\delta\boldsymbol{\theta} \tag{25}$$

The form of $\mathbf{T}(\boldsymbol{\theta})$ is given in Ibrahimbegović et al. (1995). The set of nonlinear equations is then solved with a full Newton-Raphson scheme.

Homogeneous Column, Frontal Plane Model

Linear Elastic Response

We first limit our analysis to a linear elastic response of the column. For anisotropic and homogeneous cross sections, the stress and moments are related to the strain and curvature as follows:

$$\begin{Bmatrix}\mathbf{n}^M\\ \mathbf{m}^M\end{Bmatrix}=\begin{bmatrix}\mathbf{C}_n & \mathbf{0}\\ \mathbf{0} & \mathbf{C}_m\end{bmatrix}\cdot\begin{Bmatrix}\boldsymbol{\varepsilon}^M\\ \boldsymbol{\kappa}^M\end{Bmatrix} \quad \text{where}$$

$$\begin{cases}\mathbf{C}_n=\text{diag}\left[E \quad G \quad G\right]\\ \mathbf{C}_m=\text{diag}\left[GI \quad EI \quad EI\right]\end{cases} \tag{26}$$

The quantities E, G, and I are Young's modulus, shear modulus, and moment of inertia of a circular cross section, respectively.

Muscle Response

Referring to Patwardhan et al. (2001), the muscles are assumed to behave such that they direct the load in a direction that follows the path of the vertebral column. In this work, we do not consider the moment $\bar{\mathbf{m}}_I$ exerted by muscles on the column. The action of the Ith muscle is therefore given by the force $\bar{\mathbf{f}}_I$, whose line of action is given by the unit vector $\mathbf{h}_I$. The muscle force $\bar{\mathbf{f}}_I$ is then written as

$$\bar{\mathbf{f}}_I=f_I\mathbf{h}_I \tag{27}$$

where the scalar f_I denotes the magnitude of the force $\bar{\mathbf{f}}_I$. Because muscle behaves in tension the intensity f_I is assumed to be a positive (or zero) quantity, whose value is computed by making assumptions on muscle force. In this work, we investigate two different assumptions, which lead to two models, namely, the secant model and the tangent model. Before presenting the two models, it is useful to introduce the total force $\mathbf{f}_t$ at s exerted by the portion of the column above that point. If $s=0$ denotes the bottom end of the column and $s=L$ is the top end of the column, we have

$$\mathbf{f}_t(s)=\int_s^L\left\{\rho\mathbf{g}+\sum_{I=1}^{N}\left[\bar{\mathbf{f}}_I\delta(s_I-s)\right]\right\}ds+\mathbf{t}|_{s=L} \tag{28}$$

We now introduce the two models, namely, the tangent model and the secant model. For the present study, we assume that the muscle lines of action $\mathbf{h}_I$ are all contained in the same plane (frontal plane) and that the deformation takes place in this plane. For simplicity, we consider this plane to be generated by the basis vectors $(\mathbf{e}_2,\mathbf{e}_3)$.

Tangent Model

In the tangent model, we assume that the force $\bar{\mathbf{f}}_I$ is such that the total resulting force at point s_I is tangent to the column at that point. This can be written as follows:

$$[\bar{\mathbf{f}}_I+\mathbf{f}_t(s_I)]\cdot\mathbf{m}_2=0 \tag{29}$$

In other words, the projection of the total resulting force on a direction perpendicular to the axis of the spine at s vanishes. Using Eq. (22) in Eq. (24), it is straightforward to show that

$$f_I=-\frac{\mathbf{f}_t(s_I)\cdot\mathbf{m}_2}{\mathbf{h}_I\cdot\mathbf{m}_2} \tag{30}$$

J. Eng. Mech., 2010, 136(11): 1319-1328

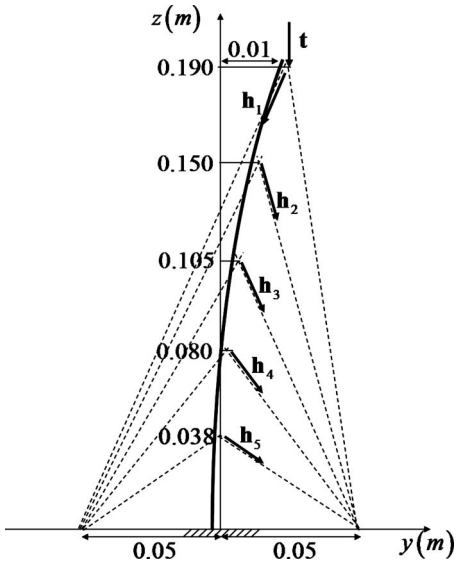

Fig. 3. Simplified model of the lumbar spine

Secant Model

In the secant model, used by Patwardhan et al. (2001), we assume that the force $\bar{\mathbf{f}}_I$ is such that the total resulting force at point s_I is directed along the vector $\mathbf{v}_I = \mathbf{x}(s_I) - \mathbf{x}(s_{I-1})$ generated by two successive muscle attachments. If we introduce $\mathbf{w}_I$ as the vector perpendicular to $\mathbf{v}_I$, we obtain the condition

$$[\bar{\mathbf{f}}_I + \mathbf{f}_t(s_I)] \cdot \mathbf{w}_I = 0 \tag{31}$$

Using Eq. (22) in Eq. (26), we obtain

$$f_I = -\frac{\mathbf{f}_t(s_I) \cdot \mathbf{w}_I}{\mathbf{h}_I \cdot \mathbf{w}_I} \tag{32}$$

Results

We first propose to investigate the frontal plane model of the lumbar spine proposed by Patwardhan et al. (2001). The model consists of the lumbar portion of the column in a flexed posture, with ten muscles (five on each side), pinned at the bottom end and subject to an increasing vertical load at the top end. The geometry of the column, muscle placement, dimensions, and boundary conditions are given in Fig. 3. The model described in Patwardhan et al. (2001) is based on a beam-column model (Timoshenko and Gere 1961) that only accounts for bending. In order to reproduce the behavior in our more general model, we used the penalty method by introducing a high elastic modulus for tension/shear and torsion modes. Referring to Eq. (21), we take the elastic parameters to be $E=G=10^9$. To reproduce the results of Patwardhan et al. (2001), the direction of muscle force $\mathbf{h}_I$ is kept constant during the simulation. Finally, similar to the study (Patwardhan et al. 2001), the secant model for the muscles' action is used.

The simulation is performed with 200 finite elements, each with one quadrature point. The top load was increased in 100-N increments and the simulation was stopped when the reaction force on the base of the column reached 1,200 N. The magnitudes of the force from right muscles and left muscles, as well as the compressive force along the column, are compared with the results of Patwardhan et al. (2001) in Fig. 4. We now propose to

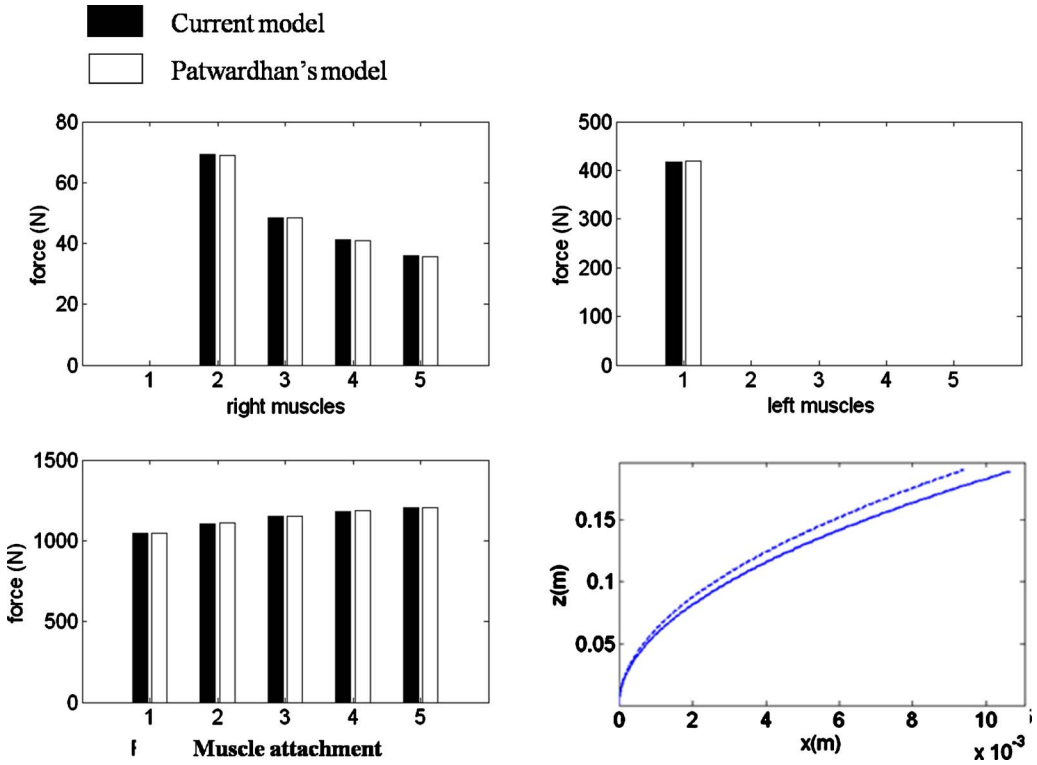

Fig. 4. Comparison of the muscle forces and reaction along the spine with the model of Patwardhan et al. (2001); the last plot shows the initial column configuration (discontinuous line) and the final configuration (solid line)

J. Eng. Mech., 2010, 136(11): 1319-1328

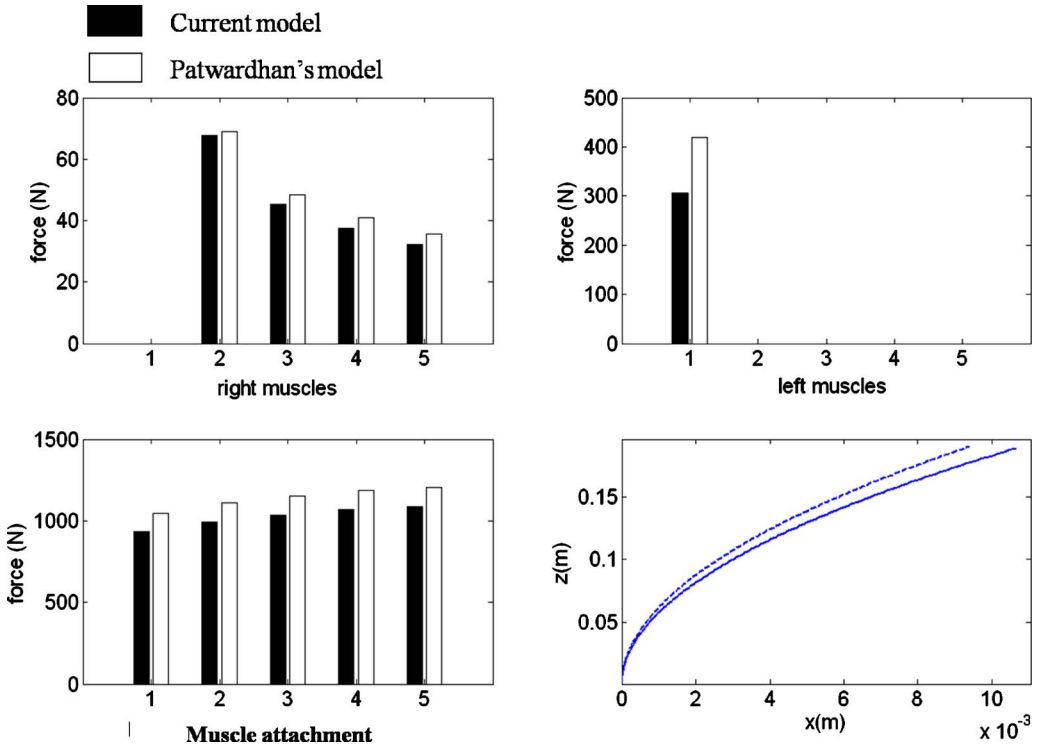

Fig. 5. Comparison of the muscle forces and reaction along the spine for the model of Patwardhan et al. (2001) and our current model, when the muscle direction is updated; the last plot shows the initial column configuration (discontinuous line) and the final configuration (solid line)

investigate various features of the new model, including nonlinear effects from the motion of muscles during deformation, the tangent model for muscles' action, and the effects of including the response of the structure in shear and tension.

Effect of Muscle Motion

Here, the direction of the muscle force $\mathbf{h}_I$ is updated as the vertebral column deforms. The muscle forces, compressive load along the column, and the deformed configuration are plotted and compared with the model of Patwardhan et al. (2001) (see Fig. 5).

Tangent Model

The tangent model for muscles' action described in the section "Tangent Model" is now investigated. As in the previous studies, the top vertical load is incremented in 100-N steps until the total compressive stress in the bottom of the column reaches 1,200 N. Referring to Fig. 6, two observations can be made: First, the difference in reaction force along the spine between the two models is not significant, and second, large differences can be seen in the column deflection (last figure) and muscles' reactions (top two figures). The tangent model requires smaller muscle forces but results in slightly larger reaction force along the spine (which relates to the compressive stress in the disks). The validity of each model may be found by experimentally monitoring the deflection of the spine under compressive load and comparing the measurements to the above results.

Nonlinear Multiscale Spine Model with Disks

The lumbar spine model is now improved as follows: First, intervertebral disks are introduced by using variable material properties in the beam. Second, the nonlinear elastic response of the disk is included while the response of vertebrae is modeled as a stiff linear elastic material. Keeping the geometry depicted in Fig. 3, five disks are introduced, centered in the midpoint between muscle attachments, as shown in Fig. 6.

Hierarchical Framework to Determine the Nonlinear Elastic Response in Bending

The mechanical response of the column is now investigated with an emphasis on bending. Other modes of deformation such as torsion, stretch, and shear are the subject of future research. The column consists of two materials.

1. The vertebrae are made of hard tissue (bone) and are considered linear elastic with a high bending stiffness.
2. The intervertebral disk structure is made of soft tissues that consist of the annulus fibrosus and the nucleus pulposus. We do not consider the effect of ligaments in this work.

The behavior and geometry of the disks are a critical factor in spine biomechanics and it is of interest to understand how mechanical properties of soft tissues can affect the overall behavior of the spinal structure. We propose a hierarchical homogenization scheme to determine the bending response of a disk, which is based on a two-step bottom-up hierarchical approach passing the information first from the fibrous structure of soft tissue to the vertebrae/disks' unit and second, from the vertebrae/disks' unit to the spine. In the first step, the mechanical response of the annulus fibrosus (present in the disk) is homogenized as an anisotropic, hyperelastic model as described in Guo et al. (2007), and the bone material is simply represented as a stiff linear elastic material. In the second step, the material model is used in a finite-element simulation of a vertebra-disk unit to generate the disk response in bending. The three-dimensional (3D) simulation is carried out with the finite-element software ABAQUS implicit using eight

J. Eng. Mech., 2010, 136(11): 1319-1328

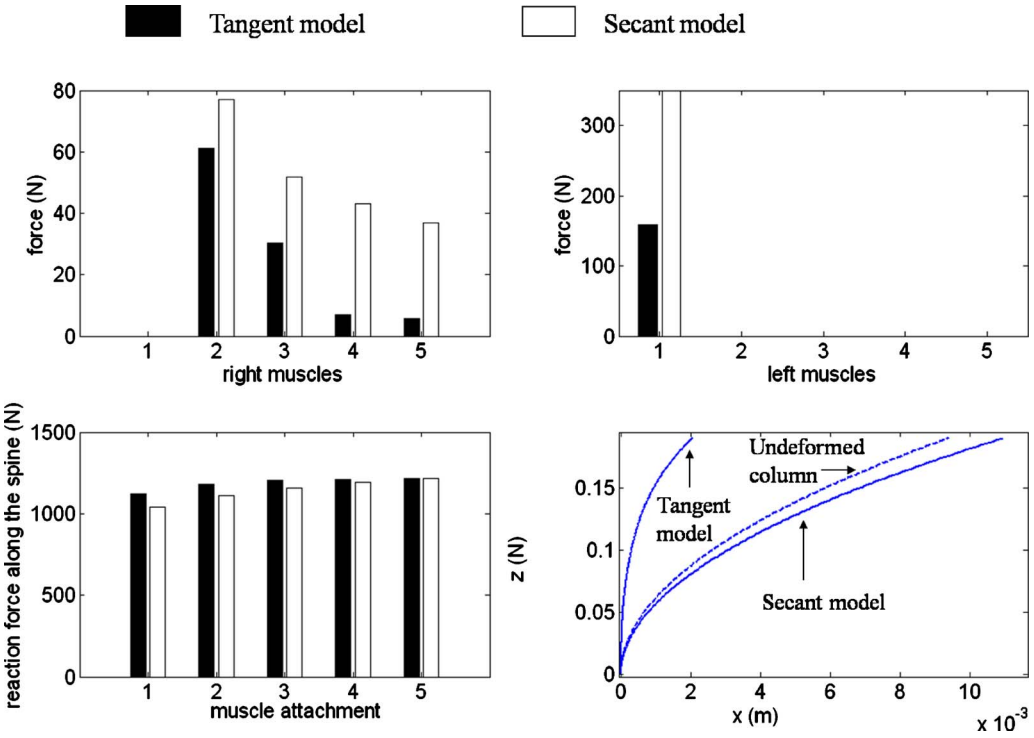

Fig. 6. Comparison of the muscle force and reaction along the spine computed with the tangent and secant model

node brick elements in the annulus and four node elements in the vertebrae. The discretization and the generated bending moment/rotation angle curve are shown in Fig. 7.

The response of the disk in bending is then determined as follows: First, we make the assumption that bending of the unit vertebra-disk-vertebra is mainly due to the disk, due to the high stiffness of the bone material. The curvature κ_d of the disk can then be written as follows:

$$\kappa_d = \frac{\Delta\theta_d}{L_d} \approx \frac{\Delta\theta_{vdv}}{L_d} \tag{33}$$

where $\Delta\theta_d$=angle difference between the top end and bottom end of the disk; $\Delta\theta_{vdv}$=angle difference between the top end and bottom end of the unit vertebra-disk-vertebra; and L_d=height of the disk. Finally, the moment-curvature curve for the intervertebral disk is determined and shown in Fig. 8. The bending stiffness of the disk is seen to increase with the level of bending strains.

Effect of the Nonlinear Disk Response

We investigate the nonlinear response of the disks and its effect on the structure. This computation is performed with both a linear and a nonlinear disk response.

Without Muscle Activation

Let us first examine the effect of the nonlinear disk response when muscles are not considered. The column is loaded at the top end, until the level of bending strain in the first disk reaches the value of 8.0 N m. The bending strains in each disk are then monitored in the final configuration and plotted in Fig. 9. Two observations can be made. First, the level of bending strains is lower when the nonlinear disk response is used. But more important, the convex stress-strain response of the nonlinear disk tends to redistribute bending strains along the spine and, as a consequence, prevents strain concentration in a single disk. This feature is important to prevent disk failure from excessive bending.

With Muscle Activation

The computation is now repeated with muscle activation. Both the secant and the tangent assumptions are considered. For both models, we plot the bending strains in the disks, the compressive force at muscle attachments, and muscle forces (Fig. 10). From the general trends in Fig. 10, one notes that large differences exist in bending curvature and muscle forces. While the compressive reaction does not differ by a significant amount, the norm of the bending curvature is significantly larger for the tangent model (for Disks 2–5). The secant model can therefore be considered a better model if the role of muscle is to minimize the strains in the intervertebral disks. However, the muscle forces for the secant model are now significantly larger than those for the secant model. Thus, the tangent model has an advantage as it is less stressful for muscles.

Discussion

By incorporating the action of muscles through the action of external forces, the developed model allows a precise and inexpensive exploration of the human spine behavior for which mechanical and geometrical properties may be easily adapted to a patient's morphology. While both the tangent and secant models for muscle force are very similar in nature, major differences are observed in the behavior of the spinal column according to the assumptions being made. This point emphasizes sensitivity of the spine behavior with respect to the model, and as a consequence, the need for a more precise description of the action of muscle. Similarly, it is shown that considering different models and assumptions can result in large differences in the macroscopic stress

J. Eng. Mech., 2010, 136(11): 1319-1328

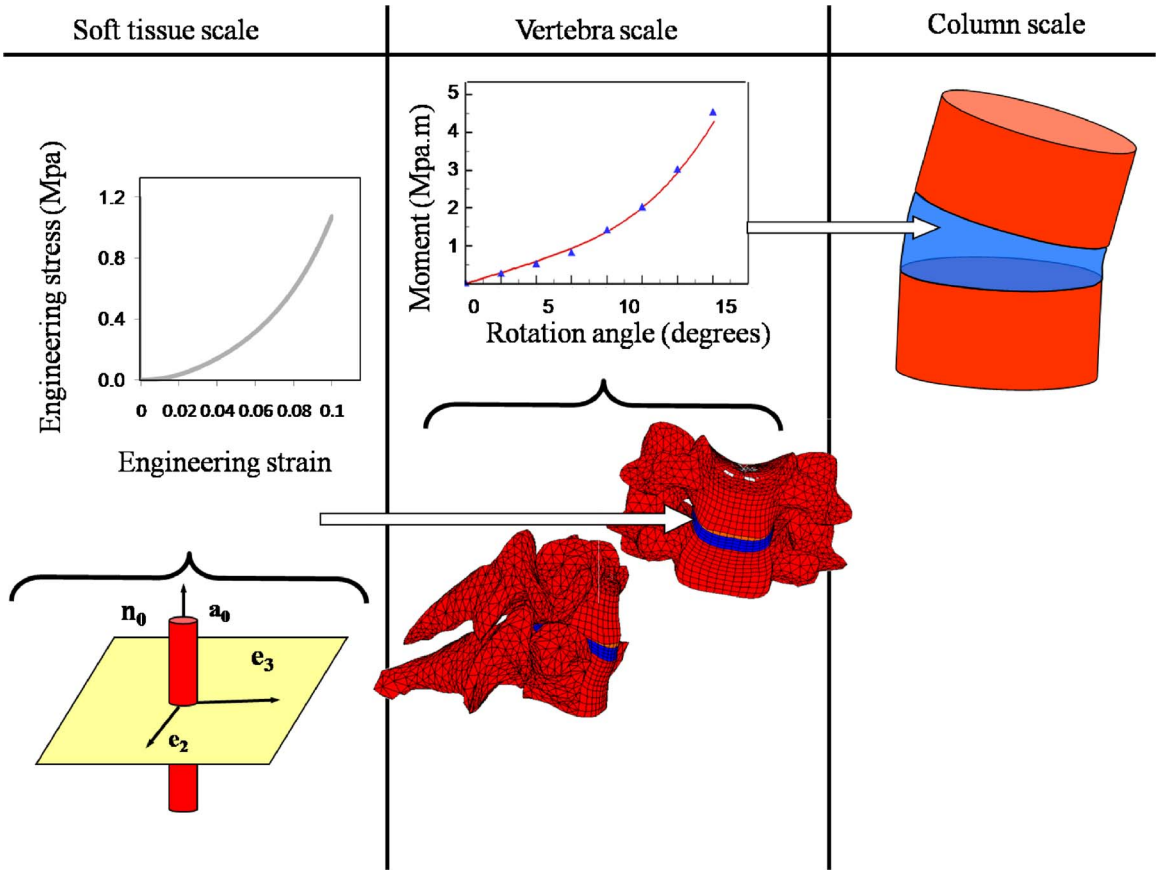

Fig. 7. Hierarchical multiscale framework to determine the response of a spine segment in bending; the soft tissue scale is represented by a composite based model (Guo et al. 2007); the vertebral scale is represented by two cervical vertebrae and a disk; the mechanical response in bending is plotted; the column scale is represented by column elements with different properties in disks and vertebrae

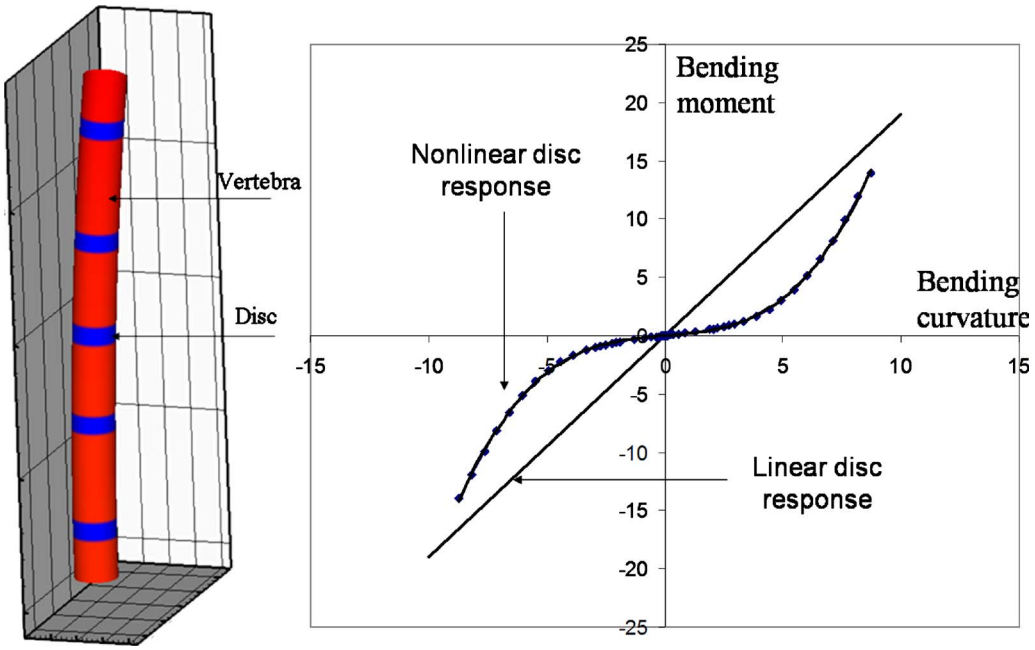

Fig. 8. 3D representation of the beam with disks and the computed moment-curvature curve for the disks; both linear and nonlinear responses are shown

J. Eng. Mech., 2010, 136(11): 1319-1328

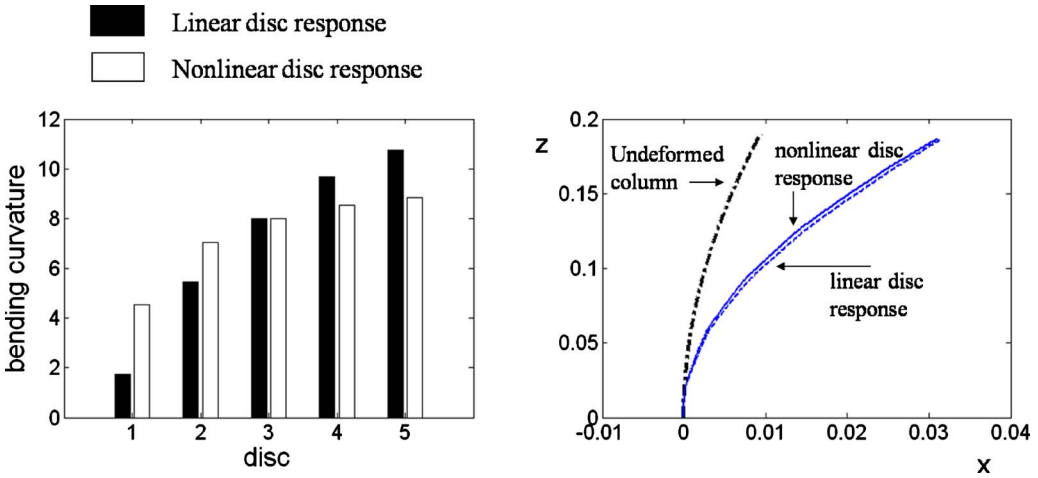

Fig. 9. Bending strains in disks for the linear and nonlinear disk responses and the corresponding final configurations

distribution, muscle forces, and spine deflection. This emphasizes the fact that due to nonlinearities both from a geometrical and material point of view, small differences at small scales might have a significant impact at the scale of the entire structure. In particular, an alteration of the disk properties due to disease or damage might have a large impact on the overall spine. The need for the multiscale modeling of the human spine is therefore reinforced.

The presented model is flexible and can be extended to describe a rich variety of spine mechanical response. Thus, the computational scheme can be enriched to include the arc-length algorithm [such as proposed in Riks (1972)] and allow detailed studies of spine instabilities (in the form of buckling, for instance). Also, while the above model is formulated under static loading condition, it can be further extended to incorporate dynamical behavior of the spine in response to high-frequency excitations. For this, the contribution of the kinetic work has to be included in Eq. (17); this will ultimately add an inertial term and a time dependency in the governing equation of the spine (Reddy 1999). In addition, experimental analysis of spine mechanics in dynamic conditions can be performed to derive assumptions regarding the dynamical response of muscles. Additional future research involves developing a constitutive response for the disks accounting for the six degrees of freedom, namely, tension, shear, bending, and torsion. The incorporation of the effects of ligaments is also an important direction for future research. The hierarchical scheme described in this study will improve our understanding of the mechanical behavior of soft tissues in the

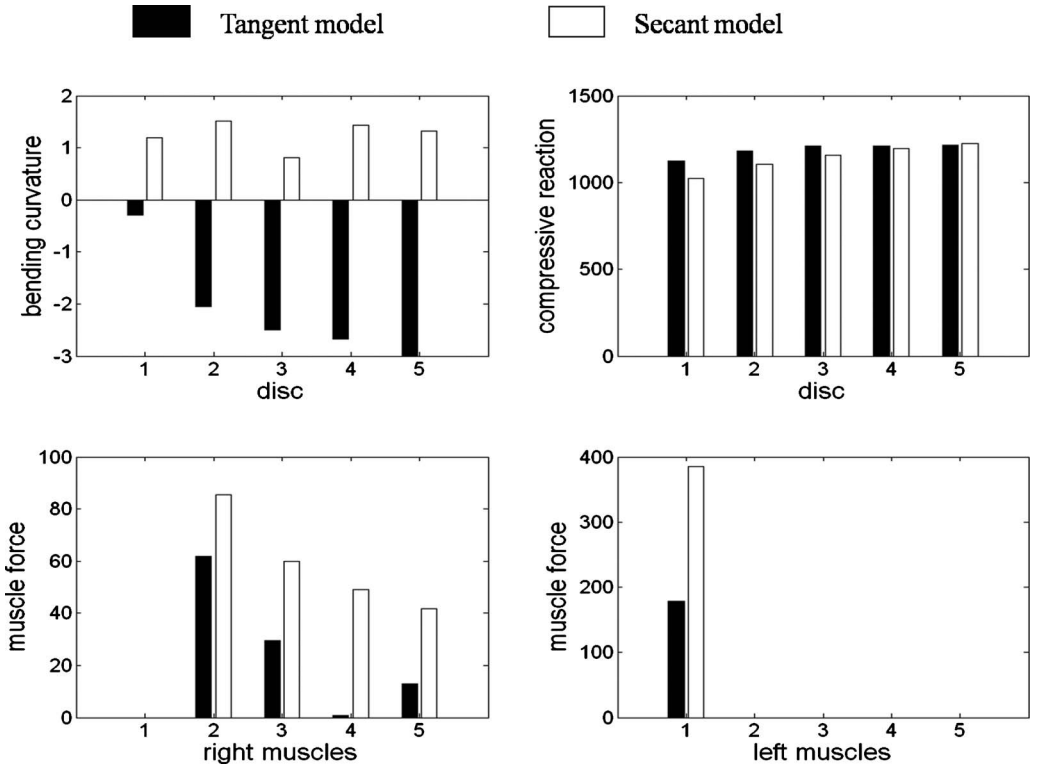

Fig. 10. Bending strains, compressive forces at disk attachment, and muscle forces for the tangent and the secant models

J. Eng. Mech., 2010, 136(11): 1319-1328

disks and ligaments in terms of their microstructure, and ultimately the behavior of the entire spine.

Acknowledgments

The writers would like to thank Medtronic-Sofamor Danek for research support.

References

Crisco, J. J., and Panjabi, M. M. (1992). "Euler stability of the human ligamentous lumbar spine. Part I: Theory." *Clin. Biomech. (Bristol, Avon)*, 7(1), 19–26.

Crisco, J. J., Panjabi, M. M., Yamamoto, I., and Oxland, T. R. (1992). "Euler stability of the human ligamentous lumbar spine. Part II: Experiment." *Clin. Biomech. (Bristol, Avon)*, 7(1), 27–32.

Guo, Z. Y., Peng, X. Q., and Moran, B. (2007). "Mechanical response of neo-Hookean fiber reinforced incompressible nonlinearly elastic solids." *Int. J. Solids Struct.*, 44(6), 1949–1969.

Hao, S., Liu, W. K., Moran, B., Vernerey, F., and Olson, G. B. (2004). "Multi-scale constitutive model and computational framework for the design of ultra-high strength, high toughness steels." *Comput. Methods Appl. Mech. Eng.*, 193, 1865–1908.

Ibrahimbegović, A., Frey, F., and Kožar, I. (1995). "Computational aspects of vector-like parameterization of three-dimensional finite rotations." *Int. J. Numer. Methods Eng.*, 38, 3653–3673.

Kapania, R. K., and Li, J. (2003). "A formulation and implementation of geometrically exact curved beam elements incorporating finite strains and finite rotation." *Comput. Mech.*, 30, 444–459.

Kiefer, A., Shirazi-Adl, A., and Parnianpour, M. (1997). "Stability of the human spine in neutral postures." *Eur. Spine J.*, 6, 45–53.

Kim, Y. H., and Kim, K. (2004). "Numerical analysis on quantitative role of trunk muscles in spinal stabilization." *JSME Int. J., Ser. C*, 47(4), 1062–1069.

Patwardhan, A. G., Meade, K. P., and Lee, B. (2001). "A frontal plane model of the lumbar spine subjected to a follower load: Implications for the role of muscles." *J. Biomech. Eng.*, 123, 212–217.

Reddy, J. N. (1999). "On the dynamic behaviour of the Timoshenko beam finite elements." *Sadhana: Proc., Indian Acad. Sci.*, 24, 175–198.

Reissner, E. (1981). "On finite deformations of space curved beams." *Z. Angew. Math. Phys.*, 32, 734–744.

Riks, E. (1972). "The application of Newton's method to the problem of elastic stability." *J. Appl. Mech.*, 39, 1060–1066.

Simo, J. C. (1985). "A finite strain beam formulation. The three-dimensional dynamic problem. Part I." *Comput. Methods Appl. Mech. Eng.*, 49, 55–70.

Simo, J. C., and Vu-Quoc, L. (1986). "A three-dimensional finite strain rod model, Part II: Computational aspects." *Comput. Methods Appl. Mech. Eng.*, 58, 79–116.

Timoshenko, S., and Gere, J. (1961). *Theory of elastic stability*, McGraw-Hill, New York.

Vernerey, F. J., and Pak, R.(2010). "On a reduced beam formulation with kinematic constraints and its application to multi-fiber systems." *J. Eng. Mech.*(under review).

Vernerey, F. J., Liu, W. K., and Moran, B. (2007). "Multi-scale micromorphic theory for hierarchical materials." *J. Mech. Phys. Solids*, 55(12), 2603–2651.